Program Digest, 2019 IEEE International Ultrasonics Symposium (IUS)
Glasgow, Scotland, October 6-9, 2019

Harmonics Amplitude in Plane and Focused Waves - a Comparative Study at Equal Mechanical Index

Francesco Guidi
Department of Information Engineering
University of Florence
Florence, Otaly
Francesco.Guidi@unifi.it

Libertario Demi
Department of Information Engineering and Computer Science
University of Trento
Trento, Italy
libertario.demi@unitn.it

Piero Tortoli
Department of Information Engineering
University of Florence
Florence, Otaly
Piero.Tortoli@unifi.it

***Abstract*—Although there is increasing interest for the use of plane waves (PWs) in high-frame-rate fundamental and harmonic imaging, no much experimental data is available about their behavior in terms of nonlinear propagation. In this paper, hydrophone measurements of PW propagation in water are presented and compared to the results obtained for focused waves (FWs) at various levels of peak negative pressure (PNP). Preliminary experiments were based on a linear array probe with 4 and 6 MHz as transmitted center frequency. The results show that the harmonics amplitudes reached by PW are generally higher than those achieved with FW at comparable PNP. At MI=0.2 the second harmonic turns out to be 8 dB higher in PW than in FW in the focal region (25 mm depth), and 20 dB higher at 40 mm depth.**

Keywords— Nonlinear propagation, plane waves, focused waves, harmonic imaging, ULA-OP

I. Introduction

Tissue Harmonic Imaging (THI) is a technique that exploits ultrasound nonlinear propagation to improve image quality. With THI, images are obtained only from the second harmonic component, which, differently from the fundamental component, is not directly transmitted by the ultrasound probe but is instead generated from tissue due to ultrasound nonlinear propagation. Several benefits can be obtained with THI over conventional ultrasound imaging, which is instead based on the fundamental component only. Particularly relevant are the improved spatial resolution, reduced side and grating lobes, and diminished clutter effects [1], [2]. Imaging with harmonics above the 2^{nd} has also been proposed in the literature to further improve the image quality [3]. This technique is known as Super Harmonic Imaging (SHI), and exploits the combination of 3^{th}, 4^{th} and 5^{th} harmonic components. The simultaneous use of multiple harmonics is necessary, as the higher is the harmonic component, the lower is the pressure-amplitude associated with it [3] even in the assumption of a lossless medium. This aspect is further highlighted by frequency dependent tissue attenuation.

Generally speaking, harmonics amplitude increases with increasing pressure amplitude associated to the transmitted ultrasound field, i.e. the fundamental component. For this reason, the use of focused waves (FWs) in transmission (TX) is considered the best choice when targeting harmonic imaging. In fact, with focused beams the peak pressure that can be generated with a given transducer array is higher than with plane or diverging wave TX, which are ideal to maximize the frame rate, another key imaging parameter [4].

However, harmonics may also be generated by nonlinear sources such as the microbubbles [5], [6] which are commonly used as contrast agents. In these cases, the transmitted pressure amplitudes are kept low to minimize the harmonic growth due to tissue nonlinearities. Plane wave (PW) imaging is thus the ideal candidate for this type of application [7], [8] as there is no need for generating strong peak pressures, while the high frame rate allows accurate evaluation of the contrast dynamics.

Harmonic amplitude is not only linked to the transmitted peak pressure amplitude or to the presence of contrast agents. It also depends on the spatial extent of the fundamental pressure field, which can be seen as a distributed source of nonlinearity. Accordingly, the combined effect of a great number of weak sources, such as with PWs, could be still greater than the effect of few strong sources, as with FWs.

In this study, we investigate harmonics growth for plane-wave and focused wave TX at equal peak negative pressure (PNP). Experimental results are reported for measurements performed in water and with varying PNP in the range used for contrast enhanced ultrasound imaging. The results show that the harmonics amplitudes reached by PW imaging are generally higher than those achieved with FWs at comparable PNP.

II. Methods

A. *Measurement system*

This study was based on the LA332 probe (Esaote, Florence, Italy) coupled to the ULA-OP open scanner [9]. The setup also includes a 6-axis positioning system with a properly synchronized hydrophone acquisition section (see fig. 1).

The LA332 is a 144-element linear array with 0.245 mm pitch, 4.6 MHz center frequency and 100% (-6 dB) bandwidth. The elements are covered by a silicon lens, which sets an elevational focus at about 23 mm.

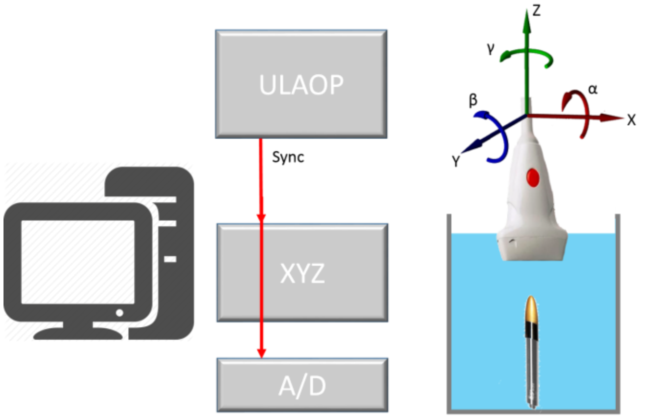

Figure 1 - Setup block diagram

The 64 central elements of the probe were excited, through the ULA-OP linear amplifiers, by Hanning weighted sinusoidal bursts at 4 or 6 MHz with 1 MHz bandwidth. The TX signals were beamformed to produce, with programmable PNP values, either FWs @ 25 mm or 35 mm, or PWs. The ultrasound beam obtained in each experimental condition was measured in water by the hydrophone moving in a volume of 20x3x40 mm. The full 3-D beam plot was thus obtained over the 10 – 50 mm depth range around the beam axis with 0.3 mm spatial resolution.

The hydrophone (Onda, mod. HGL-0400), 400 µm of electrode aperture, was connected to a low noise amplifier (Onda, mod. AH-2010) and to a 12-bit ADC sampling at 125 MSPS. The ultrasound pulses picked up by the hydrophone were acquired synchronously with the TX signals.

B. *Initial setup and data processing*

The probe was carefully oriented over the 3 angles to align the array surface with the XZ plane of the positioning system, and the acoustic axis with the hydrophone axis. The data acquired by the hydrophone were converted to Volt and then to Pascal through the hydrophone calibration curve. The data were then processed to extract the PNP values of the integral signal and, after 4° order band pass filtering, at each of the harmonics frequencies.

Preliminary acquisitions were performed in low distortion regime (MI < 0.1), to empirically equalize the PNP developed in each experimental condition, adjusting the TX signal amplitude.

III. Results

Figure 2 shows the beam-plots obtained by transmitting 6 MHz pulses with 1 MHz bandwidth to produce very low pressures in the three TX modes (FW@25 mm, 35 mm and PW). No side lobes are visible over a dynamic range > 40 dB in both FW modes.

In the second measurement step, beam-plots were acquired for two different excitation frequencies (4 and 6 MHz) and two MIs (0.1 and 0.2). Figures 3, 4 and 5 show the PNP values estimated @ 6 MHz along the probe axis. In each panel, four PNPs plots are reported: one obtained through an integral evaluation (PNP0) and the other ones obtained after filtering the first (PNP1), second (PNP2) and third (PNP3) harmonic components.

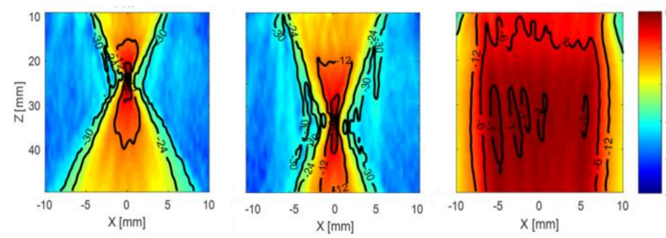

Figure 3 – Normalized PNP beam plots of FWs focused at 25mm (left) and 35 mm (center) and of PW (right) in quasi-linear conditions (MI<0.1)

Figure 3 highlights the behavior in case of close focus (25 mm). All PNPs trends show a peak at the programmed depth and a rapid decay before and after the focal depth. PNP1 closely follows the PNP0 trend at all depths, highlighting that the amount of energy reversed on the harmonics is extremely small. The harmonic contributions are below the hydrophone sensitivity threshold at small depths, they rise rapidly with depth to reach the maximum at the focal depth (PNP2 = -28 dB with respect to PNP1 for MI = 0.1 and -22 dB for MI = 0.2) and then maintain a steady distance from PNP1 at greater depths.

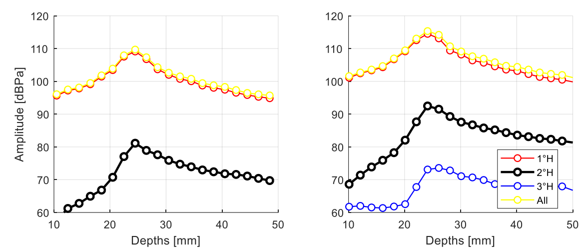

Figure 4 – Absolute PNPs in FW @ 25 mm, 6 MHz, MI = 0.1(left), 0.2 (right)

Figure 4 shows the results obtained by setting the electronic focus to 35 mm. The general trend reflects what observed in the previous case. The harmonic contributions are negligible at small depths, they quickly rise with the depth to reach peak values around the focal depth (PNP2 = -24 dB compared to PNP1 for MI = 0.1 and -17 dB for MI = 0.2). Also in this case, the harmonics levels keep steady distance from PNP1 up to greater depths. It should be noted that the maximum of harmonic

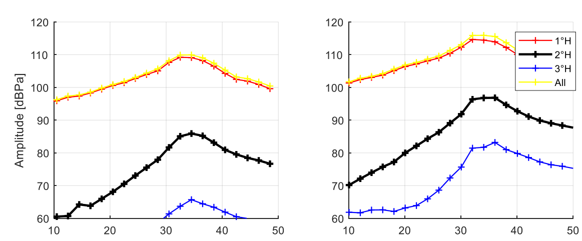

Figure 2 Absolute PNPs in FW @ 35 mm, 6 MHz, MI = 0.1(left), 0.2 (right)

contributions is here at depths slightly greater (5 mm) than the programmed depth.

A small difference between PNP0 and PNP1 is now found at MI = 0.2, showing that a small part of the acoustic energy of the signal has here shifted to the harmonic contributions.

The results obtained for PW excitation show a very different behavior with respect to the previous ones (see figure 5). Here, the PNP0 contribution tends to remain stable over a wide range of depths reaching the maximum value at about 30 mm, 7 mm beyond the natural focus of the acoustic lens. The harmonic contributions are very small near the surface of the probe but rapidly and continuously grow with depth. PNP2 reach very high values at 50 mm depth: -13 dB compared to PNP1 for MI = 0.1, and -8 dB for MI = 0.2.

The third harmonic follows the same trend and in this case rapidly assumes non-negligible values (at 50 mm depth PNP3 = -24 dB compared to PNP1 for MI = 0.1 and -14 dB for MI = 0.2). The difference between PNP0 and PNP1 is here more evident, particularly in the case of MI = 0.2.

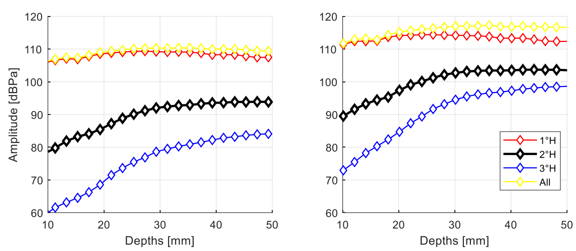

Figure 5 - Absolute PNPs in PW, 6 MHz, MI = 0.1 (left), 0.2 (right)

Figure 3, 4 and 5 compare 6 MHz harmonics components measured at low PNP targeted to ultrasound contrast agents (UCA).

At 4 MHz harmonic amplitudes were generally lower than the 6 MHz case, highlighting however very similar trends.

Table 1 - 2^{th}/ 3^{th} harmonics absolute PNP amplitudes for FW TX at 25 mm and PW TX (MI=0.2)

TX Freq. [MHz]	TX Mode	@ 25 mm [dBPa]	@ 40 mm [dBPa]
4	FW	87 / 67	78 / 61
	PW	96 / 82.5	98 / 88
6	FW	92.4 / 74	84 / 68
	PW	101 / 91	104 / 97

The table shows the 2^{th} and 3^{th} harmonics amplitude measured at two different depths (25 and 40 mm) by transmitting in FW at 25 mm or in PW, for both 4 and 6 MHz frequencies.

IV. Discussion and Conclusion

Experimental results show that the harmonics amplitude reached by PW are generally higher than those achieved with FW at comparable PNPs. Furthermore, such differences increase with depth. Absolute harmonics amplitude from PW at MI=0.1 can be even greater than absolute harmonic amplitude for FW at MI=0.2, as shown by the results for a focus at 25 mm.

This phenomenon is explainable by the combined effect of 1) the cumulative nature of the waveform steepening process and consequent increasing of the harmonics amplitude 2) the larger spatial extension of the region over which high pressure levels (in the nonlinear regime) are obtained for PW when compared to FW. In fact, PW pressure distribution is wider and more homogeneous.

Should be noticed that the high harmonics levels is well developed in a no-dissipation medium as water because it has an important nonlinearity coefficient very similar to biological tissues and has an extremely low absorption coefficient [1]. In vivo or in a standard tissue mimicking medium, the attenuation is important and frequency dependent, so the pressure profile decrease gradually with the depth, reducing the expected non-linear phenomena and potentially the differences between PW and FW.

These results can have significant impact when targeting UCA applications [10] where the generation of harmonics due to tissue nonlinearities limits the achievable contrast to tissue ratio.

References

[1] M. A. Averkiou, D. N. Roundhill, and J. E. Powers, "A new imaging technique based on the nonlinear properties of tissues," in *1997 IEEE Ultrasonics Symposium Proceedings. An International Symposium (Cat. No.97CH36118)*, 1997, vol. 2, pp. 1561–1566 vol.2.

[2] L. Demi and M. D. Verweij, "2.16 - Nonlinear Acoustics," in *Comprehensive Biomedical Physics*, A. Brahme, Ed. Oxford: Elsevier, 2014, pp. 387–399.

[3] P. L. M. J. van Neer *et al.*, "Comparison of fundamental, second harmonic, and superharmonic imaging: a simulation study," *J. Acoust. Soc. Am.*, vol. 130, no. 5, pp. 3148–3157, Nov. 2011.

[4] L. Demi, "Practical Guide to Ultrasound Beam Forming: Beam Pattern and Image Reconstruction Analysis," *Applied Sciences*, vol. 8, no. 9, p. 1544, Sep. 2018.

[5] N. de Jong, P. J. Frinking, A. Bouakaz, and F. J. Ten Cate, "Detection procedures of ultrasound contrast agents," *Ultrasonics*, vol. 38, no. 1–8, pp. 87–92, Mar. 2000.

[6] F. Guidi, H. Vos, R. Mori, N. de Jong, and P. Tortoli, "Microbubble characterization through acoustically-induced deflation," *IEEE Transactions on Ultrasonics, Ferroelectrics, and Frequency Control*, vol. 57, pp. 193–202, 2010.

[7] J. Viti, H. J. Vos, N. D. Jong, F. Guidi, and P. Tortoli, "Detection of Contrast Agents: Plane Wave Versus Focused Transmission," *IEEE Transactions on Ultrasonics, Ferroelectrics, and Frequency Control*, vol. 63, pp. 203–211, 2016.

[8] F. Guidi, O. Supponen, A. Upadhyay, H. J. Vos, M. A. Borden, and P. Tortoli, "Microbubble radiation force-induced translation in plane-wave versus focused transmission modes," *IEEE Transactions on Ultrasonics, Ferroelectrics, and Frequency Control*, pp. 1–1, 2019.

[9] P. Tortoli, L. Bassi, E. Boni, A. Dallai, F. Guidi, and S. Ricci, "ULA-OP: An Advanced Open Platform for Ultrasound Research," *IEEE Transactions on Ultrasonics, Ferroelectrics, and Frequency Control*, vol. 56, pp. 2207–2216, 2009.

[10] P. Palanchon, P. Tortoli, A. Bouakaz, M. Versluis, and N. de Jong, "Optical observations of acoustical radiation force effects on individual air bubbles," *IEEE Transactions on Ultrasonics, Ferroelectrics, and Frequency Control*, vol. 52, no. 1, pp. 104–110, Jan. 2005.